1 **FEASIBILITY OF COUPLING PERMEABLE BIO-BARRIERS AND**

2 **ELECTROKINETICS FOR THE TREATMENT OF DIESEL**

3 **HYDROCARBONS POLLUTED SOILS**

4

5 Esperanza Mena Ramírez[2], Cristina Sáez Jiménez[1,3], José Villaseñor Camacho[2,*],

6 Manuel A. Rodrigo Rodrigo[1,3] and Pablo Cañizares Cañizares[3]

7

8 (1) ISE member

9 (2) Chemical Engineering Department. Research Institute for Chemical and

10 Environmental Technology (ITQUIMA). University of Castilla La Mancha, 13071,

11 Ciudad Real, Spain.

12 (3) Chemical Engineering Department. Faculty of Chemical Sciences and Technology.

13 University of Castilla La Mancha, 13071, Ciudad Real, Spain.

14 *Corresponding author. Tel.: +34 926295300; E-mail: Jose.Villasenor@uclm.es

15

16 **Abstract**

17 In this study, the remediation of a diesel hydrocarbon-polluted clay soil using an

18 electrochemical-biological combined technology is assessed. The polluted soil was

19 subjected to an electrokinetic (EK) treatment with a biological permeable reactive

20 barrier. A lab-scale electrochemical cell for soil treatment was used. The biological

21 barrier placed in the soil was a biofilm reactor previously adapted for diesel

22 degradation. A batch experiment of 336 h was conducted in a synthetic clay soil spiked

23 with 10 g·kg$^{-1}$ of diesel and a constant voltage gradient of 1.0 V cm$^{-1}$. Sodium dodecyl

24 sulphate was used as an anionic surfactant in the cathodic well to allow for hydrocarbon

25 emulsification during the treatment. At the end of the experiment, extreme pH values

26  were observed near the electrodes. However, the pH remained constant at

27  approximately 7.7 in the central biobarrier zone, which allowed for biological processes.

28  Biological growth was observed in the biobarrier, and a part of the biofilm was detached

29  and transported through the soil in both directions. Furthermore, the surfactant was

30  transported across the soil due to electromigration and electroosmosis, which resulted in

31  diesel emulsification. The combination of biological and EK phenomena finally

32  resulted in a homogenous hydrocarbon removal of approximately 27% in the polluted

33  soil, which indicated a 39% removal of the diesel biodegradable fraction.. Due to the

34  electroosmotic flow and the biological degradation, some of the water, surfactant and

35  inorganic nutrients were removed from the soil and should be continuously replaced if a

36  long-time experiment is conducted.

37

41

## 1. Introduction

The electrokinetic (EK) treatment of polluted soils consists of applying a low intensity direct electric current through the soil between appropriately distributed electrodes. Consequently, different EK phenomena (electromigration, electrophoresis and electroosmosis) occur in the soil when a current is applied, which promotes the transport of ionic and molecular species in the soil, including pollutants, microorganisms or nutrients, and leads to *in situ* soil remediation. Generally, EK technology is specifically recommended for the treatment of low permeability clay soils [1-5]. In the recent years, interest has increased in combining the advantages of EK technologies with other conventional soil remediation technologies to improve remediation efficiency [6]. In particular, one possible technique is the combination of permeable reactive barriers (PRB) and EK treatments *in situ*.

Generally, PRBs are engineered zones of a reactive material that is placed in the direction of groundwater flow to help intercept a pollution plume that is carried within an aquifer by retaining or degrading the pollutants [7]. The subsurface pollution plume can be caused to flow through the PRB using the natural hydraulic gradient or a pump-and-treat method. However, when the soil to be treated has very low permeability properties, the mobilization of the water using this conventional technique is not possible. Thus, when a PRB is coupled with EK technology, the pollutants are driven by the EK mass transport processes described above.

Different materials could be used to build different PRBs that are based on several different mechanisms (reduction using elemental metals, adsorption with porous high-surface materials, ion exchange with resin-based materials, biological degradation, etc.). In particular, barriers based on biological degradation are named biological permeable reactive barriers (Bio-PRB) or biobarriers. A biobarrier is a fixed culture bioreactor that

67    includes a porous supporting material and a microbial biofilm attached on its surface.

68    The working principle of a biobarrier is the same as that of a conventional biofilm

69    reactor. In fact, the only difference is that it is inserted in the soil during EK treatment.

70    Numerous publications are available regarding the use of PRBs [8-13] or biobarriers

71    [14-20] for the removal of heavy metals or organic compounds from polluted soils.

72    However, the combination of the EK and the PRB treatments is much more recent, and

73    consequently, only a limited number of publications are available regarding this topic:

74    some studies are based on using physical and/or chemical mechanisms in the PRB to

75    remove metals or organic pollutants [21-27], while, to our knowledge, no references are

76    available regarding the specific case of combined biological barriers/EK treatment. The

77    combination of biotechnology and the EK phenomena for polluted soils remediation has

78    been called "electrobioremediation" and has been previously studied as another strategy

79    [2, 28-40].

80    In this study, a soil polluted with diesel hydrocarbons is treated using the EK/Biobarrier

81    method. Hydrocarbon soils and groundwater pollution are major environmental

82    problems that are usually caused by a number of anthropogenic activities that are

83    inefficient or by uncontrolled accidents (leaking tanks or ruptured pipelines at service

84    stations or in industrial areas). In this paper, we propose applying the EK/PRB

85    remediation technology by using a biobarrier with a diesel degrading microbial

86    consortia attached on the surface of gravel particles. Because diesel composition is a

87    complex mixture of different hydrocarbons, diesel fuel could be used as a model for

88    studying the treatment of this type of pollution in soils. The most relevant difference

89    between this study and previous studies is the innovative combination of the biobarrier

90    and the EK process for remediating soil polluted with diesel-oil.

91

## 2. Experimental

### 2.1. Electrokinetic installation

The lab-scale set-up is shown in Figure 1, and was made of transparent methacrylate and divided into five compartments. The central compartment contained the polluted soil in which the biobarrier with the diesel degrading support microorganism was loaded. The pore system of the biobarrier was filled with a Bushnell Hash Broth (BHB) inorganic nutrient solution, a commercial inorganic nutrient salt mixture that was specific for heterotrophic microbial development and was provided by Difco$^{TM}$ (Le Pont de Claix, France). The BHB composition was as follows: 0.2 g·l$^{-1}$ MgSO$_4$, 0.02 g·l$^{-1}$ CaCl$_2$, 1.0 g·l$^{-1}$ KH$_2$PO$_4$, 1.0 g·l$^{-1}$ (NH$_4$)$_2$HPO$_4$, 1.0 g·l$^{-1}$ KNO$_3$ and 0.05 g·l$^{-1}$ FeCl$_3$. The diesel-polluted soil was loaded on both sides of the biobarrier and separated from it by 0.5 mm nylon mesh. The biobarrier was 5 cm thickness. The two electrodic compartments were located on one side of each section of the polluted soil and were separated from the soil by 0.5 mm nylon mesh. One of these compartments served as an anodic well, and the other compartment served as a cathodic well. Each electrodic compartment was finally connected to an additional collector compartment at both extremes to collect the liquid that overflowed from the electrodic wells. Graphite electrodes were introduced in the electrodic compartments and were connected to the power supply device (HQ Power, Gavere, Belgium) so that one of them served as the anode and the other served as the cathode. The electrodes had dimensions of 10.0 × 10.0 × 1.0 cm and were provided by Carbosystem (Madrid, Spain). To obtain a homogeneous distribution of current lines throughout the soil, the electrodes were positioned to cover the same cross section as the fraction of the soil to be studied. The system was open in the top side in order to reproduce a possible future full scale application.

## 2.2. Materials

Electrochemical techniques are especially recommended for treating low permeability soils, such as clays. Therefore, in this study, kaolinite (provided by Manuel Riesgo Chemical Products, Madrid, Spain) was used as a model for clay soil. The properties of this synthetic clay soil are detailed in Table 1.

The diesel oil that was used as the pollutant was a conventional petroleum-derived fuel that was purchased from a petrol station in Ciudad Real, Spain. In previous characterization tests [41] using chromatography analysis, it was determined that the n-alkanes that were predominantly present in the commercial oil had chain lengths of between 10 and 26 carbon atoms. In addition, pristane and phytane biomarkers were identified. The density of the diesel was $882 \text{ g·l}^{-1}$ when measured according to a standard procedure (ISO-3675 1998).

To artificially pollute the soil, the diesel was diluted tenfold in acetone before evenly distributing the solution drop by drop in the corresponding amount of kaolinite. The solvent (acetone) and the higher volatile diesel fractions (approximately 6% of the initial amount of added diesel) were allowed to evaporate at room temperature for at least two days. The concentration of diesel present in the soil at the beginning of the experiment was approximately $10 \text{ g·kg}^{-1}$.

## 2.3. Biobarrier development

The gravel support was used for the biobarrier with a particle diameter of approximately 4 mm. The following procedure was used to develop the biobarrier with the attached diesel-degrading biofilm: first, the gravel bed was immersed in a BHB solution with a small amount of diesel ($2.1 \text{ g·l}^{-1}$) that was emulsified with the sodium dodecyl sulphate (SDS) surfactant ($1.0 \text{ g·l}^{-1}$) that was provided by Panreac Chemical Products (Barcelona, Spain). In turn, microorganisms that were previously acclimated to diesel

142    degradation [41] were inoculated into the flooded bed. Under these conditions, the

143    culture was allowed to grow for one week to allow the microorganisms attached on the

144    gravel surface to develop. Once this first activation period expired, a feed pump was

145    connected to the system so that the BHB medium including the diesel emulsified with

146    SDS passed through the gravel bed. The diesel concentration in the medium was

147    approximately 2.1 $g \cdot l^{-1}$ (an approximate value of 4.0 $g \cdot l^{-1}$ if expressed as the Chemical

148    Oxygen Demand, COD). The bed was continuously flooded with no aeration such that

149    the input of the feed solution was performed in the bottom of the reactor that contained

150    the developing biobarrier and the output occurred through an overflow. The feed flow

151    was set so that the residence time in the reactor was approximately 4 h, which was the

152    optimum value according to previous studies that were conducted with the same

153    microbial culture [41]. During the steady state operation of the system, a total COD

154    removal efficiency of more than 50% was achieved (data not shown). This removal

155    included the COD due to the diesel and the surfactant. SDS is an organic compound that

156    is derived from the C-12 alkane and can be easily biodegraded by the diesel-degrading

157    microbial consortia. In fact, in a previous test, more than 95% of the surfactant was

158    degraded in 7 days of operation. Consequently, a diesel-removing biofilm reactor was

159    developed for use as a biobarrier.

160    **2.4.  Experimental procedure**

161    The soil was manually compacted into the central compartment on both sides of the

162    biobarrier to achieve the highest degree of compaction possible and avoid the formation

163    of preferential flow paths that could interfere with the results. The bulk dry density of

164    the soil after compaction was approximately 1300 $Kg \ m^{-3}$. Next, the biobarrier was

165    loaded into the central position (Figure 1) and flooded with the BHB medium. An

166    inorganic salts mixture was used as an anolyte and to moisten the soil and ensure

167   electrical conductivity. This salt solution was composed of the following: 30.36 mg·l$^{-1}$

168   of NaNO$_3$, 70 mg·l$^{-1}$ of NaHCO$_3$ and 88.75 mg·l$^{-1}$ of Na$_2$SO$_4$. The clay soil was wetted

169   to obtain saturated conditions to a moisture content of approximately 40% (0.4 kg water

170   per kg of wet soil). On the other side and in the cathodic compartment, an anionic

171   surfactant solution was used as a catholyte. A 2.38 g·l$^{-1}$ SDS solution was loaded into

172   the cathodic compartment at the beginning of the the experiment.

173   The experiment was performed using a potentiostatic method (i.e., setting a voltage

174   gradient value that remained constant throughout the experiment). The current intensity

175   values varied with time and depending on the characteristics of the medium. In this

176   case, the voltage gradient was set at 1.0 V·cm$^{-1}$. Based on the length of the treated

177   section (20 cm), the total value of the fixed voltage was 20 V.

178   **2.5.   Sampling and analyses**

179   The duration of the experiment was two weeks, and the following parameters were

180   monitored daily: temperature and the dissolved oxygen (DO) concentrations in the

181   biobarrier liquid medium; the electrical current trough the soil (using a multimeter that

182   was capable of measuring the electrical current in milliamps); the electro-osmotic water

183   volume that was collected in the cathodic compartment; and the pH, conductivity and

184   total-P, total-N, diesel and SDS concentrations in the electro-osmotic water that were

185   mobilized, in the anolyte, catholyte and in the liquid biobarrier medium. In addition, the

186   following parameters were measured in the soil at the beginning and end of the

187   experiment: pH, conductivity, moisture content, the concentration of microorganisms

188   and the total-P, total-N, diesel and SDS concentrations. At the end of the experiment,

189   both sections of the polluted soil were divided into eight portions, so that the parameter

190   measurements were performed at 16 points in the soil. Thus, the influence of the

191  position of the electrode on the measured parameters were analysed in addition to the

192  axial deviation at the points that were situated at the same distances as the electrodes.

193  Next, the analytical procedures for the measurement of each parameter are detailed. The

194  humidity was calculated in the soil samples by accounting for the loss in mass after

195  drying at 105°C for 24 h. The pH, conductivity and the total P, total N, diesel and SDS

196  concentrations were measured from the soil samples as follows: 10 g of the dried soil

197  samples were suspended in 25 ml of Milli-Q water using 20 min of vigorous magnetic

198  agitation. Next, the samples were centrifuged at 4000 rpm for 15 min. The parameters

199  were measured in the supernatant phase. The pH was measured using a CRISON pH

200  meter and the conductivity was measured using a Jenway conductivimeter. In addition,

201  the dissolved oxygen (DO) concentration in the biobarrier liquid medium was measured

202  using a Hanna 98186 selective electrode. The N and P concentrations were measured

203  using a Gallery photometric analyser (Thermo Fischer Scientific, Massachusetts, USA).

204  The SDS concentration was measured using a previously reported specific photometric

205  method [42, 43]. Briefly, 5 ml of the sample was alkalinized by adding 200 μl of a 50

206  mM sodium tetraborate solution. Next, 100 μl of a stabilized methylene blue solution

207  was added to the sample and homogenized. Finally, 4 ml of chloroform was added.

208  After vigorous stirring for 30 s followed by 5 min at rest, the absorbance of the organic

209  phase was measured at 650 nm.

210  Diesel hydrocarbons concentration was expressed as Total Petroleum Hydrocarbon

211  (TPH) measured by GC-FID. Taking into account the amount of diesel in the soil at the

212  beginning of the experiments and the results obtained in the analysis of the soil samples

213  at the end of the experiments, the total amount of diesel removed from the system was

214  calculated, following the same procedure previously detailed in bibliography [44]. The

215  diesel concentrations were determined using a fractionated serial extraction as follows:

216    10 g of wet soil were mixed with 6 ml of hexane (divided into three steps of 2 ml). In

217    every single step extraction, the soil was mixed with the corresponding volume of

218    dissolvent and agitated vigorously in a Vortex agitator for 5 min. Next, the samples

219    were centrifuged at 4000 rpm for 15 min. The samples that were taken from the organic

220    supernatant phase were analysed using a Trace GC Ultra (Thermo Fisher Scientific,

221    Massachusetts, USA) gas chromatograph that was equipped with a flame ionization

222    detector (GC-FID). The hydrocarbons were separated in a micro Ultra Fast capillary

223    column (5 m × 0.1 mm i.d. × 0.4 μm). The injector and the detector were scheduled at a

224    temperature of 250ºC and 280ºC, respectively, and the thermal ramps used were as

225    follows: initial temperature of 65°C for 0.1 min. followed by a gradient of $50ºC·min^{-1}$

226    until a final temperature of 70ºC to be maintained during 1.5min., after that another

227    gradient of $180ºC·min^{-1}$ until a final temperature of 240ºC maintained during 2 min.,

228    and finally, another gradient of $250ºC·min^{-1}$ until a final temperature of 280ºC

229    maintained for 1 min. The carrier gas used was high purity helium, whit a flow of 50

230    $ml·min^{-1}$. Finally, the injection volume was 1 μL and a split injection mode was

231    employed.

232    The concentration of microorganisms was expressed in Colony Forming Units (CFU)

233    per gram of dry soil and was measured by suspending 10 g of wet soil in 10 ml of saline

234    water  using 1 min of Vortex agitation. Next, an aliquot of 100 μL of the soil-saline

235    suspension was plated on Petri dishes. The nutrient solid phase of these dishes was

236    prepared using LB medium (with the following composition per litre of deionised

237    water: 10 g NaCl, 5 g yeast extract and 10 g casein peptone) with 15 $g·l^{-1}$ of European

238    Bacteriological Agar and 2 $g·l^{-1}$ of glucose as the carbon source. Inoculums were evenly

239    spread using Digralsky handles, and the plates were incubated for 48 h at 26°C, which

240    provided sufficient time for enumerating the individual colonies that were present in

241   each sample. Finally, the biomass concentrations in the biobarrier were determinate

242   before and after the treatment. This value corresponds to the weight difference of the

243   dried samples before and after calcination at 550°C for 2 h.

**3. Results and Discussion**

245   Figure 2 shows the pH and conductivity profiles of the soil after treatment.

246   As expected due to the water electrolysis reactions, an acidic pH was obtained in the

247   areas near the anode electrode. In addition, a basic pH was obtained near the cathode

248   electrode (Figure 2, part a). Because the rate at which protons ions move through the

249   soil is greater than the rate at which hydroxyl ions move through the soil, the changes in

250   the baseline value to an acidic pH in the areas near the anode were more pronounced

251   than the changes in the baseline value to a more basic pH in the areas near the cathode.

252   The soil conductivity was greater in the areas closer to the anode and lower near the

253   cathode (Figure 2, part b). This result occurred because the basic pH caused

254   precipitation and fixed the ionic species. Thus, the mobility of the ionic species was

255   more limited. Conversely, the increase in the conductivity in the area near the anode

256   resulted from the electromigration of the anions and the liberation of the species due to

257   the influences of the acidic pH front.

258   Figure 3 shows the experimental conditions in the biobarrier during the experiment. All

259   of the conditions were adequate for the biological degradation of diesel during the

260   experiments. The temperature was slightly above room temperature because the heat

261   caused by the application of the electric field was not pronounced, but was slightly

262   below the optimum value for the microbial consortium used, which was 26°C [41]. In

263   the last hours of the experiment, the temperature decreased, which corresponded with

264   the accentuated decrease in the electrical current that was obtained at the same time.

265   The pH values stayed approximately constant at neutral position throughout the

266     experiment. The influences of the acid and the basic fronts were neutralized in the

267     centre of the soil section where the biobarrier was installed, and thanks to the buffer

268     effect of the biological growth liquid medium. The DO concentration increased to a

269     value near the saturation point (6 ppm). Due to the salinity of the system, this value

270     must be below the value that was obtained for the pure water (approximately 8 ppm).

271     The DO concentration near the saturation conditions was maintained nearly constant

272     throughout the experiment. In addition, it has been supposed that the electro-osmotic

273     flow could cause the drag of the oxygen generated at the anode surface through the soil.

274     The previous development of the microorganisms attached in the biobarrier was

275     conducted under flooded and non-aerated conditions. Thus, in its application for soil

276     treatment, high dissolved oxygen concentrations would not be necessary for the diesel

277     biodegradation process. However, aerobic processes are usually more efficient, which

278     could be relevant for the application of this technology in similar aerobic remediation

279     processes.

280     Figure 4 shows the variations in the electric current intensity with time during the

281     experiment. Decreasing electrical currents resulted from the removal of ionic species

282     from the soil solution. This removal is due to the electromigration phenomena

283     throughout the soil and causes the accumulation of the anionic and cationic species in

284     the anodic and cathodic compartments, respectively, and also due to precipitate

285     formation in the higher pH region. In the same way, the electroosmotic drag can result

286     in the removal of the ionic water-soluble species from the system. These EK mass

287     transport processes removed the ionic species from the soil and decreased the

288     conductivity.

289     Figure 5, part a, shows the concentrations of the viable microorganisms in the soil at the

290     beginning and end of the experiment at the different sampling points. Please note that

291    the horizontal dashed line in figure 5a indicates just the initial microorganisms

292    concentration in the central biobarrier, because there were no microorganisms in the soil

293    at the beginning of the experiment. At the end of the experiment, higher microbial

294    concentrations were observed in the central areas near the biobarrier in which the diesel

295    degrading microorganisms were supported (Figure 5.a). In this area (as previously

296    discussed), conditions are optimal for microbial growth in terms of the pH and nutrient

297    concentrations. Similarly, in the areas near the electrodes, the microbial concentrations

298    were lower. Indeed, a possible experimental error in certain measurements should be

299    considered (point 1, upper right position). In these zones, the conditions for microbial

300    growth became more extreme as the experiment progressed, especially regarding the pH

301    values and the inorganic nutrient availability. Moreover, the presence of

302    microorganisms in zones that were far from the central biobarrier resulted from the

303    biofilm detachment process and the EK transport of the microorganisms [45]. The

304    biofilm detachment process resulted from biomass growth and the movement of water

305    through the biobarrier.

306    The results shown in Figure 5. b indicated that an homogeneous removal of pollutants

307    was achieved in the soil (approximately 27% of diesel was removed from the soil).

308    Because the higher volatile hydrocarbon fractions were previously removed and the

309    increase in soil temperature was negligible, hydrocarbon volatilization was not

310    considered, and only the combination of biological and EK phenomena was assumed to

311    be responsible for the diesel removal. Moreover, no diesel oil was detected in the

312    electrodic wells. The homogeneity of the diesel removal would result from two aspects.

313    First, the microorganisms were present nearly throughout the soil portion (not only the

314    biobarrier) due to the biofilm detachment and the EK transport. In addition, the diesel

315    could be emulsified with SDS and moved across the soil because a combination of

316   electrokinetic phenomena (later discussed in figures 6 and 7) and it would allow for the

317   mobilization of the diesel through the biobarrier, where higher degradation activity

318   would be conducted. When comparing a previous study regarding diesel biodegradation

319   with the same microbial consortia [40] and the removal of diesel that was obtained

320   during the biobarrier development in the present work (data not shown), the

321   biodegradable fraction of the COD of the diesel that was used was approximately 70%.

322   This result indicates that an important amount of the biodegradable fraction of the diesel

323   hydrocarbons (39% approximately) were removed trough the EK/biobarrier treatment in

324   two weeks.

325   Figure 6, part a, shows the surfactant profile that was obtained in the soil at the end of

326   the experiment. Surfactant was not added in the soil at the beginning of the experiment,

327   but 500 ml of a 2.38 $g \cdot l^{-1}$ SDS solution was added in the cathodic well. At the end of the

328   experiment, the surfactant was distributed throughout the soil according to the data

329   presented in Figure 6.a, and reached higher concentrations in the areas near the cathodic

330   well where the surfactant was introduced at the beginning of the experiment. The

331   surfactant was mobilized by electromigration from the cathode to the anode

332   compartment because it was an anionic product. Thus, small amounts of the surfactant

333   were detected in the anodic well with time, and the surfactant concentrations decreased

334   in the cathodic well as the experiment progressed (Figure 6.b). It is hypothesised also

335   that micelles, which are soluble in water, were dragged by the electroosmotic process

336   from the anode to the cathode. The combination of electromigration towards the anode

337   and electroosmosis towards the cathode would produce the movement of SDS/diesel

338   micelles across the whole soil, passing through the biobarrier in both directions.

339   Previous research [46] reported similar movement of hydrocarbons emulsified with

340   flushing fluids in EK experiments. Thus, due to the contributions of the EK and

14

341    biological phenomena, a SDS distribution across the soil was obtained to help with

342    homogeneous pollutant removal (as explained above). It is important to note that a

343    certain amount of surfactant would be biodegraded by the microbial consortia, which

344    agrees with the results that were obtained during the biobarrier development. According

345    to the mass balance calculation, 267 mg of SDS were removed from the soil by

346    biodegradation, which corresponds to approximately 22% of the total amount of

347    surfactant that was added to the system at the beginning of the experiment. In addition,

348    the surfactant biodegradation and replacement should be considered in the long-term

349    experiments.

350    Furthermore, the total volatile solids concentrations in the biobarrier were measured.

351    This concentration was directly related to the biomass concentration that was supported

352    in the biobarrier. Overall, the amount of biomass attached to the biobarrier increased by

353    25% after the process (from an initial value of 5.93 $mg \cdot kg^{-1}$, to a final value of 7.50

354    $mg \cdot kg^{-1}$). Again, this result confirmed the presence of biological activity in the area of

355    the biobarrier that caused the biological degradation of the pollutant.

356    As noted in Figure 7, the average value of the obtained electro-osmotic flow was 8.8

357    $ml \cdot h^{-1}$. Thus, after 335 h of the experiment, a volume of approximately 2500 ml of

358    water was mobilized by the electro-osmotic process towards the cathode. Considering

359    that the volume of the pore water in the soil at the beginning of the experiment was

360    approximately 1040 ml, the volume of water that was moved by electro-osmosis was

361    2.5 times greater than the volume of the pore water in the soil under saturated

362    conditions. Therefore, the influences of the electro-osmotic phenomena on the drag of

363    the species in the soil are important. In addition, a water balance was calculated and

364    indicated that water was removed from the system by evaporation at a rate of

365    approximately 3.2 $ml \cdot h^{-1}$. Considering that the electroosmotic flow was 8.8 $ml \cdot h^{-1}$, the

366   amount of water flowing vertically was 36% of the amount of water flowing

367   horizontally. In our case, approximately 1060 ml of water was lost by evaporation from

368   the system, which is a very remarkable value when considering that the water volume in

369   the soil at the beginning of the experiment was 1040 ml. Therefore, the influences of

370   vertical fluxes must be considered in this process, especially in systems where the

371   vertical dimension is predominant.

372   Finally, the nutrient availability for biological processes, and the possible pH changes in

373   the biobarrier in longer experimental periods, must be considered. Due to the

374   combination of the biological and EK phenomena, the initially high total-N and total-P

375   concentrations (500 and 300 mg·l$^{-1}$, respectively) strongly and quickly decreased in the

376   biobarrier zone. The observed average removal rates from the biobarrier zone were

377   approximately 27 mg $NO_3^-$ l$^{-1}$ d$^{-1}$, 33 mg $NH_4^+$ l$^{-1}$ d$^{-1}$ and 16 mg $PO_4^{3-}$ l$^{-1}$ d$^{-1}$, which

378   caused that  the biological growth medium was continuously replaced in the biobarrier

379   in order to avoid rate limitations because of lack of nutrients. The bioavailability of the

380   nutrients in this type of soil under the EK conditions was previously reported [47].

381   Approximately 495 mg of N and 290 mg of P need to be replaced in the system during

382   the removal of approximately 27% of the hydrocarbon (expressed as COD). Also, it

383   must be noted that after two weeks the centre soil section was still neutral but it is

384   possible that the proton mobility could affect in longer experimental periods and cause

385   pH decrease. Thus, the biological growth medium replacement also included a buffer

386   solution to avoid strong pH changes.

387

388

389

390

## 4. Conclusions

Although the EK treatment caused pH variations near the electrodes, the pH remained neutral in the central biobarrier area, thanks to the buffer effect of the biological growth liquid medium, which was adequate for the biological process. Important biological growth was observed in the biobarrier, the amount of biomass attached increased by 25% after the process, and part of the biofilm was detached. The EK transport processes caused the surfactant and the excess biomass distribution across the soil. Consequently, the combination of electromigration towards the anode and electroosmosis towards the cathode would produce the movement of SDS/diesel micelles across the whole soil, passing through the biobarrier in both directions, which resulted in a homogeneous hydrocarbon removal of approximately 39% of the diesel biodegradable fraction in 336 h. The water, surfactant and inorganic nutrients were partially removed from the soil, which should be continuously replaced to maintain adequate experimental conditions. The economical applicability of this proposed technology would depend on the analysis of the electrical power consumption and nutrient supply costs, compared to the cost savings because of the in situ technique.

## 5. Acknowledgments

## 6. Author Disclosure Statement

The authors declare no competing financial interest.

## 7. References

[1] K.R. Reddy, C. Cameselle, Electrochemical Remediation Technologies for Polluted Soils, Sediments and Groundwater, John Wiley & Sons, Inc., Hoboken, New Jersey, 2009.

416 [2] H.I. Gomes, C. Dias-Ferreira, A.B. Ribeiro, Electrokinetic remediation of

417 organochlorines in soil: Enhancement techniques and integration with other remediation

418 technologies, Chemosphere 87 (2012) 1077-1090.

419 [3] E.G. Sumbarda-Ramos, O.X. Guerrero-Gutierrez, B. Murillo-Rivera, I. González,

420 M.T. Oropeza-Guzman, Electrokinetic treatment for clayed and sandy soils, J. Appl.

421 Electrochem. 40 (2010) 1255-1261.

422 [4] R.E. Saichek, K.R. Reddy, Electrokinetically enhanced remediation of hydrophobic

423 organic compounds in soils: A review, Crit. Rev. Env. Sci. Tech. 35 (2005) 115-192.

424 [5] A.T. Lima, P.J. Kleingeld, K. Heister, J.P.G. Loch, Removal of PAHs from

425 contaminated clayey soil by means of electro-osmosis, Sep. Purif. Technol. 79 (2011)

426 221-229.

427 [6] A.T. Yeung, Y.Y. Gu, A review on techniques to enhance electrochemical

428 remediation of contaminated soils, J. Hazard. Mater. 195 (2011) 11-29.

429 [7] E.K. Nyer, In situ treatment technology, Lewis Publishers, Boca Raton, Florida,

430 2001.

431 [8] R. Focht, J. Vogan, S. O'Hannesin, Field application of reactive iron walls for in-situ

432 degradation of volatile organic compounds in groundwater, Remediation J. 6 (1996) 81-

433 94.

434 [9] A.R. Gavaskar, Design and construction techniques for permeable reactive barriers,

435 J. Hazard. Mater. 68 (1999) 41-71.

436 [10] B.D.M. Painter, Reactive Barriers: Hydraulic Performance and Design

437 Enhancements, Ground Water 42 (2004) 609-617.

438 [11] M.M. Scherer, S. Richter, R.L. Valentine, P.J.J. Alvarez, Chemistry and

439 Microbiology of Permeable Reactive Barriers for In Situ Groundwater Clean up, Crit.

440 Rev. Microbiol. 26 (2000) 221-264.

441  [12] F.G. Simon, T. Meggyes, T. Tünnerrneier, K. Czurda, K.E. Roehl, Long-term

442  behaviour of permeable reactive barriers used for the remediation of contaminated

443  groundwater, in: Proceedings of the 8 th International Conference on Radioactive Waste

444  Management and Environmental Remediation ICEM, 2001, p. 637.

445  [13] R. Thiruvenkatachari, S. Vigneswaran, R. Naidu, Permeable reactive barrier for

446  groundwater remediation, J. Ind. Eng. Chem. 14 (2008) 145-156.

447  [14] C.M. Kao, S.C. Chen, J.K. Liu, Development of a biobarrier for the remediation of

448  PCE-contaminated aquifer, Chemosphere 43 (2001) 1071-1078.

449  [15] C.M. Kao, S.C. Chen, J.Y. Wang, Y.L. Chen, S.Z. Lee, Remediation of PCE-

450  contaminated aquifer by an in situ two-layer biobarrier: Laboratory batch and column

451  studies, Water Res. 37 (2003) 27-38.

452  [16] S.J. Liu, B. Jiang, G.Q. Huang, X.G. Li, Laboratory column study for remediation

453  of MTBE-contaminated groundwater using a biological two-layer permeable barrier,

454  Water Res. 40 (2006) 3401-3408.

455  [17] H.Q. Ma, L.Y. Zhang, H.L. Zhang, S. Li, In situ remediation of petroleum

456  hydrocarbon contaminated groundwater using a novel biobarrier, Chongqing Daxue

457  Xuebao/Journal of Chongqing University 34 (2011) 99-104.

458  [18] K.D. Miller, P.C. Johnson, C.L. Bruce, Full-scale in-situ biobarrier demonstration

459  for containment and treatment of MTBE, Remediation J. 12 (2001) 25-36.

460  [19] S. Saponaro, M. Negri, E. Sezenna, L. Bonomo, C. Sorlini, Groundwater

461  remediation by an in situ biobarrier: A bench scale feasibility test for methyl tert-butyl

462  ether and other gasoline compounds, J. Hazard. Mater. 167 (2009) 545-552.

463  [20] S. Saponaro, A. Careghini, L. Romele, E. Sezenna, A. Franzetti, I. Gandolfi, M.

464  Daghio, G. Bestetti, Remediation of groundwater polluted by gasoline-derived

465  compounds with biobarriers, WIT Trans. Ecol. Envir. 164 (2012) 439-449.

466    [21] H.I. Chung, M. Lee, A new method for remedial treatment of contaminated clayey

467    soils by electrokinetics coupled with permeable reactive barriers, Electrochim. Acta 52

468    (2007) 3427-3431.

469    [22] L. Cang, D.M. Zhou, D.Y. Wu, A.N. Alshawabkeh, Coupling electrokinetics with

470    permeable reactive barriers of zero-valent iron for treating a chromium contaminated

471    soil, Separ. Sci. Technol. 44 (2009) 2188-2202.

472    [23] Y.C. Huang, Y.W. Cheng, Electrokinetic-enhanced nanoscale iron reactive barrier

473    of trichloroethylene solubilized by Triton X-100 from groundwater, Electrochim. Acta

474    86 (2012) 177-184.

475    [24] Z. Li, S. Yuan, J. Wan, H. Long, M. Tong, A combination of electrokinetics and

476    Pd/Fe PRB for the remediation of pentachlorophenol-contaminated soil, J. Contam.

477    Hydrol. 124 (2011) 99-107.

478    [25] C. Ruiz, E. Mena, P. Cañizares, J. Villaseñor, M.A. Rodrigo, Removal of 2,4,6-

479    Trichlorophenol from Spiked Clay Soils by Electrokinetic Soil Flushing Assisted with

480    Granular Activated Carbon Permeable Reactive Barrier, Ind. Eng. Chem. Res. 53 (2013)

481    840-846.

482    [26] J. Wan, Z. Li, X. Lu, S. Yuan, Remediation of a hexachlorobenzene-contaminated

483    soil by surfactant-enhanced electrokinetics coupled with microscale Pd/Fe PRB, J.

484    Hazard. Mater. 184 (2010) 184-190.

485    [27] C. Yuan, T.S. Chiang, The mechanisms of arsenic removal from soil by

486    electrokinetic process coupled with iron permeable reaction barrier, Chemosphere 67

487    (2007) 1533-1542.

488    [28] G.V. Chilingar, W.W. Loo, L.F. Khilyuk, S.A. Katz, Electrobioremediation of soils

489    contaminated with hydrocarbons and metals: Progress report, Energ. Source. 19 (1997)

490    129-146.

491    [29] Z.-Y. Dong, W.-H. Huang, D.-F. Xing, H.-F. Zhang, Remediation of soil co-

492    contaminated with petroleum and heavy metals by the integration of electrokinetics and

493    biostimulation, J. Hazard. Mater. 260 (2013) 399-408.

494    [30] M.J. Harbottle, G. Lear, G.C. Sills, I.P. Thompson, Enhanced biodegradation of

495    pentachlorophenol in unsaturated soil using reversed field electrokinetics, J. Environ.

496    Manage. 90 (2009) 1893-1900.

497    [31] T. Li, S. Guo, L. Zhang, F. Li, Electro-biodegradation of the oil-contaminated soil

498    through periodic electrode switching, in: Proceedings of the 4th International

499    Conference on Bioinformatics and Biomedical Engineering iCBBE, 2010, Article

500    number 5517376.

501    [32] F. Li, S. Guo, N. Hartog, Electrokinetics-enhanced biodegradation of heavy

502    polycyclic aromatic hydrocarbons in soil around iron and steel industries, Electrochim.

503    Acta 85 (2012) 228-234.

504    [33] Q. Luo, H. Wang, X. Zhang, X. Fan, Y. Qian, In situ bioelectrokinetic remediation

505    of phenol-contaminated soil by use of an electrode matrix and a rotational operation

506    mode, Chemosphere 64 (2006) 415-422.

507    [34] X. Fan, H. Wang, Q. Luo, J. Ma, X. Zhang, The use of 2D non-uniform electric

508    field to enhance in situ bioremediation of 2,4-dichlorophenol-contaminated soil, J.

509    Hazard. Mater. 148 (2007) 29-37.

510    [35] Q. Luo, X. Zhang, H. Wang, Y. Qian, The use of non-uniform electrokinetics to

511    enhance in situ bioremediation of phenol-contaminated soil, J. Hazard. Mater. 121

512    (2005) 187-194.

513    [36] X. Mao, J. Wang, A. Ciblak, E.E. Cox, C. Riis, M. Terkelsen, D.B. Gent, A.N.

514    Alshawabkeh, Electrokinetic-enhanced bioaugmentation for remediation of chlorinated

515    solvents contaminated clay, J. Hazard. Mater. 213-214 (2012) 311-317.

516    [37] J.L. Niqui-Arroyo, M. Bueno-Montes, R. Posada-Baquero, J.J. Ortega-Calvo,

517    Electrokinetic enhancement of phenanthrene biodegradation in creosote-polluted clay

518    soil, Environ. Pollut. 142 (2006) 326-332.

519    [38] J.L. Niqui-Arroyo, J.J. Ortega-Calvo, Integrating biodegradation and

520    electroosmosis for the enhanced removal of polycyclic aromatic hydrocarbons from

521    creosote-polluted soils, J. Environ. Qual. 36 (2007) 1444-1451.

522    [39] L.Y. Wick, L. Shi, H. Harms, Electro-bioremediation of hydrophobic organic soil-

523    contaminants: A review of fundamental interactions, Electrochim. Acta 52 (2007) 3441-

524    3448.

525    [40] S. Suni, E. Malinen, J. Kosonen, H. Silvennoinen, M. Romantschuk,

526    Electrokinetically enhanced bioremediation of creosote-contaminated soil: Laboratory

527    and field studies, J. Environ. Sci. Heal. A  42 (2007) 277-287.

528    [41] E. Moliterni, R.G. Jiménez-Tusset, M. Villar Rayo, L. Rodriguez, F.J. Fernández,

529    J. Villaseñor, Kinetics of biodegradation of diesel fuel by enriched microbial consortia

530    from polluted soils, Int. J. Environ. Sci. Te. 9 (2012) 749-758.

531    [42] K. Hayashi, A rapid determination of sodium dodecyl sulfate with methylene blue,

532    Anal. Biochem. 67 (1975) 503-506.

533    [43] E. Jurado, M. Fernández-Serrano, J. Núñez-Olea, G. Luzón, M. Lechuga,

534    Simplified spectrophotometric method using methylene blue for determining anionic

535    surfactants: Applications to the study of primary biodegradation in aerobic screening

536    tests, Chemosphere 65 (2006) 278-285.

537    [44] E. Moliterni, L. Rodriguez, F.J. Fernández, J. Villaseñor, Feasibility of different

538    bioremediation strategies for treatment of clayey and silty soils recently polluted with

539    diesel hydrocarbons, Water, Air, and Soil Pollution 223 (2012) 2473-2482.

540 [45] E. Mena, J. Villasenor, P. Canizares, M.A. Rodrigo, Influence of soil texture on the

541 electrokinetic transport of diesel-degrading microorganisms, Journal of Environmental

542 Science and Health - Part A Toxic/Hazardous Substances and Environmental

543 Engineering 46 (2011) 914-919.

544 [46] J. Kim, K. Lee, Effects of electric field directions on surfactant enhanced

545 electrokinetic remediation of diesel-contaminated sand column, Journal of Environmental

546 Science and Health - Part A Toxic/Hazardous Substances and Environmental Engineering

547 34 (1999) 863-877.

548

549 [47] E. Mena, J. Villaseñor, M.A. Rodrigo, P. Cañizares, Mobility and bioavailability of

550 nutrients and microbial electron acceptors in bioelectroremediation processes in soils,

551 in: A.N. Alshawabkeh (Ed.), 12th International Symposium on Electrokinetic

552 Remediation, Northeastern University, Boston, MA, USA, 2013, p. 49.

553

554

555

556

557

558

559

560

561

562

563

564

565

Anodic Compartment

Collector Compartment

Power Supply

A    V

Multimeter

mA

Electrolite

Level Control

Cathodic Compartment

Polluted Soil   Bio-PRB   Polluted Soil

10cm.

10cm.

20 cm.

Electrosmotic volume

Graphite electrode Anode

Graphite electrode Cathode

Collector Compartment

a

Right

Left

Upper

Bottom

Polluted Soil

Polluted Soil

Anode (+)    1         2      Bio-PRB    3         4    Cathode (-)

b

566

567

**Figure 1**

25
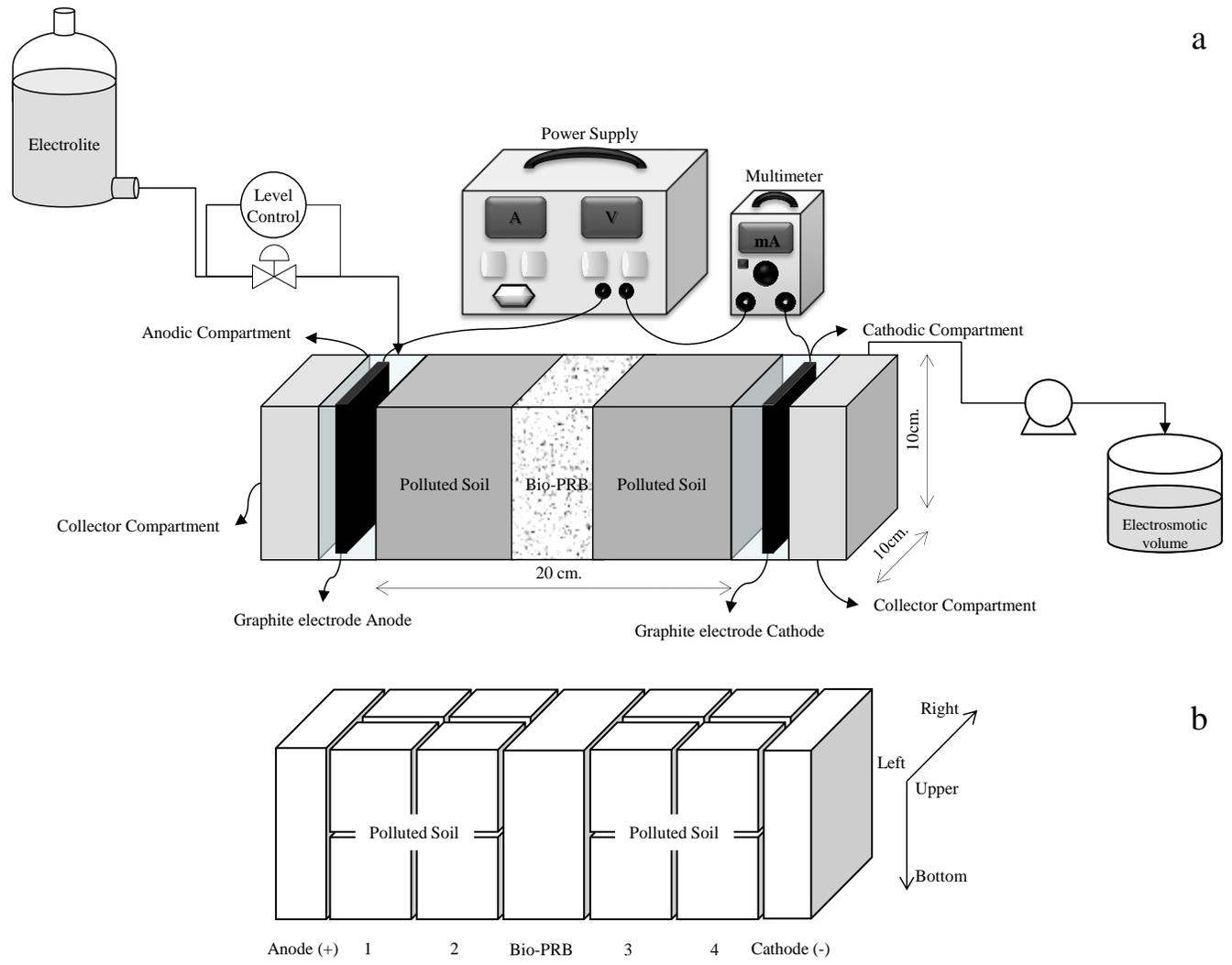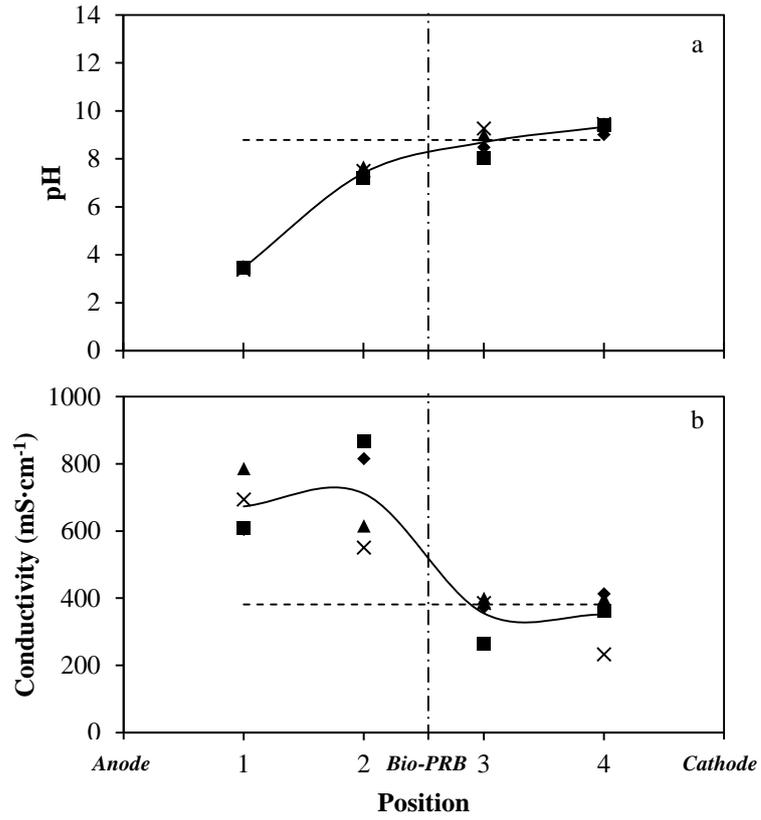
568

569

570

571

572

573

574

575

576

577

578

579

580

581                                              **Figure 2**
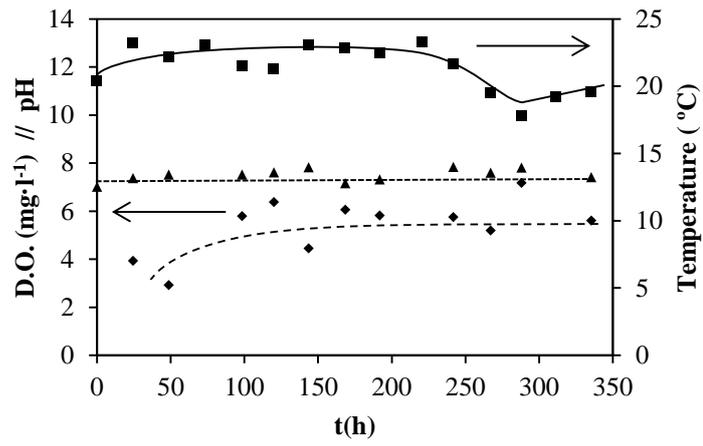
582

583

584

585

586

587

588

589

590

591

592

593

594

595

596

597

598

599

600 **Figure 3**
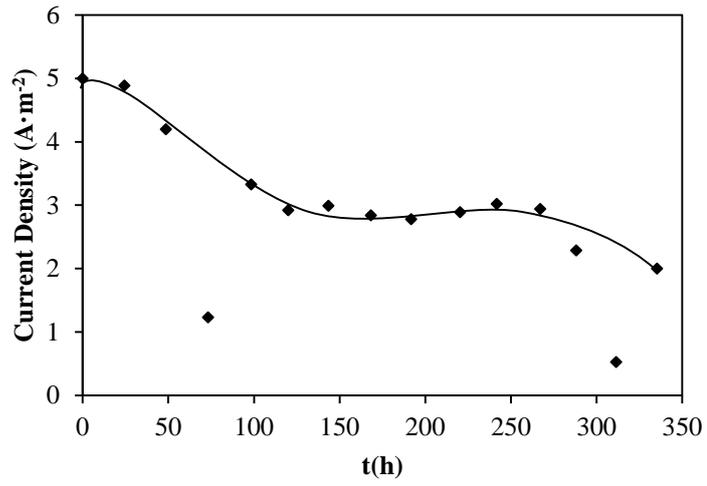
601

602

603

604

605

606

607

608

609

610

611

612

613

614

615

616

617

618

619                                                    **Figure 4**
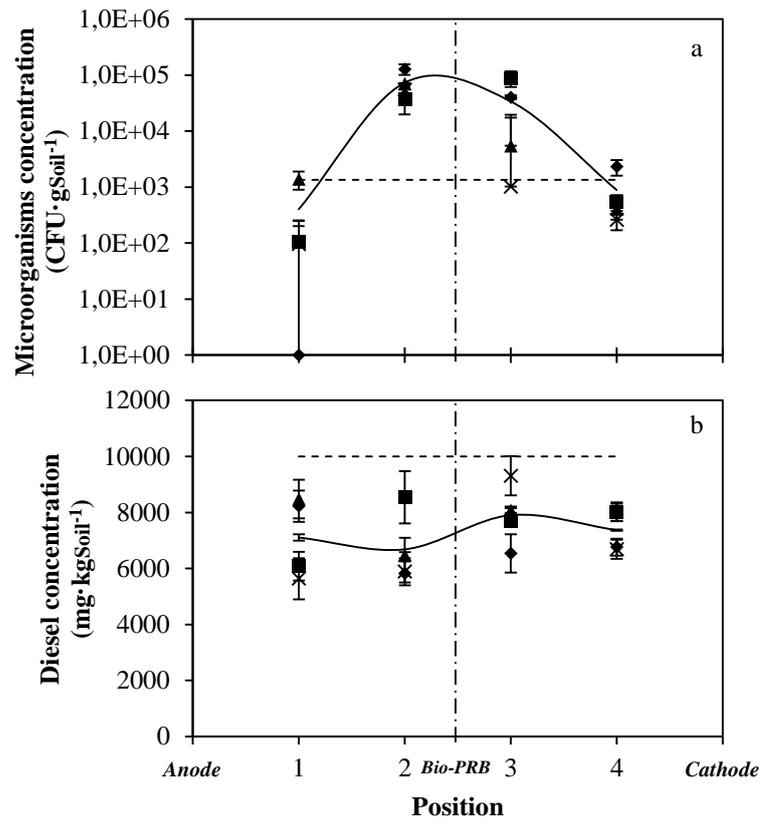
**Figure 5**

620

621

622

623

624

625

626

627

628

629

630

631

632

633
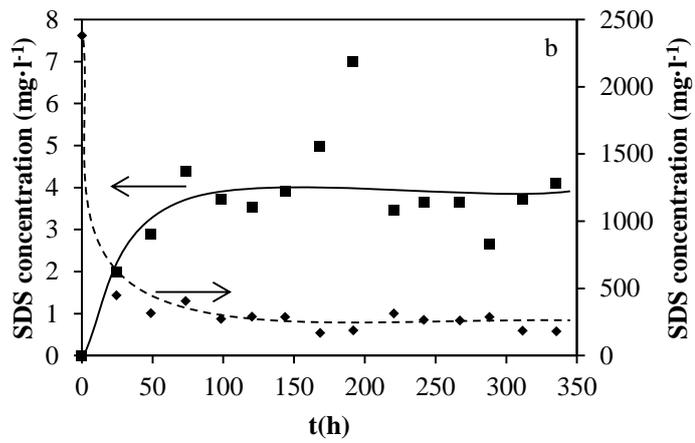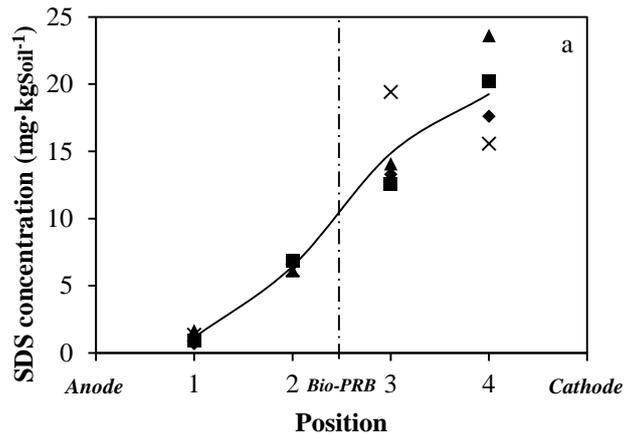
634

635

636

637

638

639

640

641

642

643

644

645

646                                    **Figure 6**
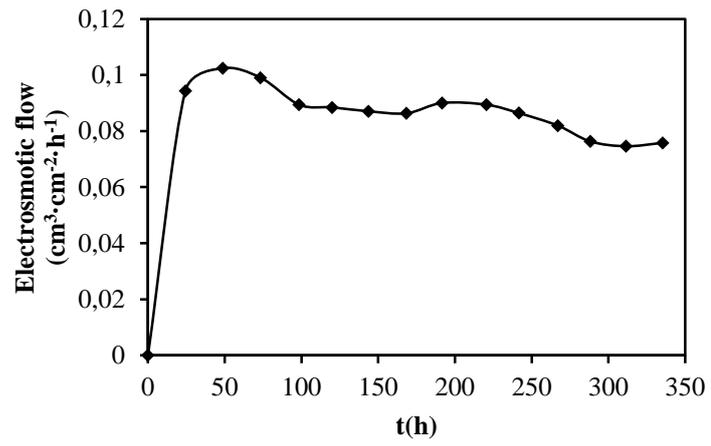
Figure 7

647

648

649

650

651

652

653

654

655

656

657

658

659

660

661

662

663

664

665